



ISSN 1110-0451



(E S N S A)

Using Beryllium-7 as a Natural Radionuclide for Assessing Short-term Soil Erosion in Arid Agricultural Land, Egypt

M. F. Kassab¹, A. Hegazi¹, M. Salem¹, M. Benmansour²

⁽¹⁾ Department of Soils and Water Research, Nuclear Research Center, Egyptian Atomic Energy Authority, Cairo, Egypt

⁽²⁾ Centre National de l'Énergie des Sciences et Techniques Nucléaires (CNESTEN), Rabat, Morocco

ARTICLE INFO

Article history:

Received: 22nd Aug. 2021

Accepted: 23rd Nov. 2021

Keywords:

Soil erosion,

Beryllium-7,

Fallout radionuclide,

Gamma spectrometry.

ABSTRACT

The use of ⁷Be as a natural tracer for estimating soil erosion has been demonstrated as a promising tool. Erosion assessment was carried out using ⁷Be technique at an arid area of Egypt, located 35 km from Cairo upon a rain event of 54mm. The technique estimates soil erosion and deposition due to rainfall event by comparing ⁷Be activity concentration at a reference site and eroded or depositional sites. Soil samples were collected from three fields with different land uses, uncultivated, prickly pear field (*Opuntia*) and olives field (*Olea europaea*). The ⁷Be in the reference site was observed in the upper 14 mm of soil surface, the reference ⁷Be inventory value was 124 ± 30 Bq.m⁻². ⁷Be inventories of the uncultivated field was lower than the reference inventory and ranged from 59.9 to 122.5 ± 30 Bq.m⁻². The ⁷Be inventories in prickly pear field ranged from 89.5 to 296.6 ± 30 Bq.m⁻² showing erosion at upslope and deposition downslope in each field, a similar behavior was observed at olives field where ⁷Be inventories ranged from 73.9 to 263.6 ± 30 Bq.m⁻². Net soil erosion rates of 37, 4.1 and 17.9 (t. ha⁻¹) were estimated for uncultivated soil, Prickly pear and olives, respectively. Combining these results with visual observations at the three fields reveals that the main driving force of the soil erosion and deposition processes by rain water was the hillslope topography. From the assumptions of applied technique, we can conclude that it gives robust evaluation of soil erosion due to rainfall.

INTRODUCTION

Soil erosion by water is an important environmental problem in today's world. More than 75% of the surface land area affected by erosion is located in developing countries in Africa, Asia and Latin America, with about 50% in Asia [1], and about 12% of the land area in the European Union is threatened by water erosion [2]. The annual cost of soil loss is estimated to be US \$400 billion per year [3, 4].

Successful applications of environmental radionuclides such as ¹³⁷Cs, ²¹⁰Pb and ⁷Be for evaluating soil erosion and deposition have been confirmed worldwide [1, 5–9].

In the Mediterranean region and particularly in arid areas, soils are very susceptible to risks of erosion, due

to the rainfall regime (sometimes an intensive rainfall) which can cause extensive runoff events amplified by hillslope topography [10]. To meet the food demand, due to population increase and deterioration in soil productivity, it becomes essential to cultivate land inappropriate for agriculture [11]. Soil erosion by wind is more common in the Egyptian deserts. However heavy and intensive rain events can happen due to the climate change extreme events causing soil erosion by water leading to removing the top fertile soil layer and causing land degradation.

High-cost investments are required to combat soil erosion; hence it should be oriented to critical areas and time period during the most vulnerable season, therefore, comprehensive knowledge of spatial and temporal

variability of erosion processes is essentially needed. Gaining reliable information is, however, challenging. Conventional methods for measuring soil erosion are labor-intensive and time-consuming, and data need to cover several decades to get a good representation of mean erosion rates. Furthermore, most conventional methods (except for geodetic method) do not provide information on the spatial distribution of erosion. [12]

Isotope tracers can help meet these deficiencies as some radionuclides and stable isotopes occurring in the environment can serve as environmental tracers and hence facilitate the investigation of these landscape processes.

Beryllium-7 (^7Be) is formed in the atmosphere and it is a cosmogenic radionuclide resulting from the cosmic ray spallation with nitrogen and oxygen atoms [13–16].

About three quarters of ^7Be is formed in the stratosphere and the remaining quarter in the upper troposphere [17]. The ^7Be fallout took place with precipitation and removing it from the air, and its deposition was found high during the summer and low during the winter due to the activity distributions of ^7Be and ^{210}Pb and the climate conditions [18]. Beryllium-7 is transported to ecosystems primarily as Be^{2+} with rainfall. As Be^{2+} ions interact with soils and vegetation, they are rapidly trapped by cation exchange surfaces [19]. In environmental samples, the ^7Be is easily deduced by gamma spectrometry using its photopeak at 477.6 keV.

The distribution of ^7Be concentration over a certain area is fundamentally uniform at a given time [20]. The main advantages of ^7Be for surveying environmental processes are its continuous production rate, short half-life and it can be detected easily by gamma spectrometry. It is highly adsorbed to fine particles [21], which are expected to be subjected to mobilization in hillslope systems.

The ^7Be technique was successfully applied for estimating soil redistribution processes associated with individual events of heavy rain at scales ranging from plot size up to field scale [6, 17, 22–29]. Kaste et al. [30] demonstrated that most of the ^7Be erosion assessment were carried out in wet conditions having moderate or a well-balanced supply of moisture, and there is a deficiency of published work in arid environments where there are potential challenges in terms of Be-7

sorption behavior under infiltration excess overland flow conditions [21, 22].

In general, soil erosion and/or deposition rates are assessed using fallout radionuclides through comparing the inventories of the areas subjected to erosion or deposition with a reference plot.

In the present research, ^7Be was used for the first time in Egypt to assess the potential for Be-7 to estimate soil erosion caused by intensive rain event over a range of contrasting land use practices. We evaluated soil erosion in an area located in an arid zone where uncultivated and cultivated areas were investigated.

MATERIALS AND METHODS

Site Description and Field Conditions

The study area is located at the experimental farm of the Nuclear Research Center, Atomic Energy Authority, Egypt. The site is situated at $30^{\circ}17'52''\text{N}$, $31^{\circ}24'34''\text{E}$ respectively, while the altitude is 20 m above the sea level. The soil texture of study area is classified as a sandy soil (Table 1) and it was divided into three successive fields along the direction of the slope, the first field is uncultivated and its slope is approximately 2.7 % while the second and third fields are cultivated with prickly pears and olives respectively and its slopes approximately are 2.3 and 2.6 respectively as indicated in Figure (1). The prickly pears farm was cultivated in 2015 and the olives farm was established in 2000. Both farms are irrigated by the drip irrigation system. The study area located in an arid climate zone according to Knöppen classification.

The annual average rainfall in the study area based on historical data is about 27 mm per year. On 11th and 12th March 2020, the area was subjected to a relatively intensive rain event, about 54 mm was recorded by meteorological station located in the study area with a maximum intensity of $50\text{ mm}\cdot\text{hr}^{-1}$. Composite soil samples were collected from the study area on March, 24th, 2020,

The precipitation is the main source of ^7Be , therefore it is essential to continuously monitor the rainfall data as it is the main driving force of erosion. Figure (2) shows the sum of daily precipitation and daily average, maximum and average air temperature.

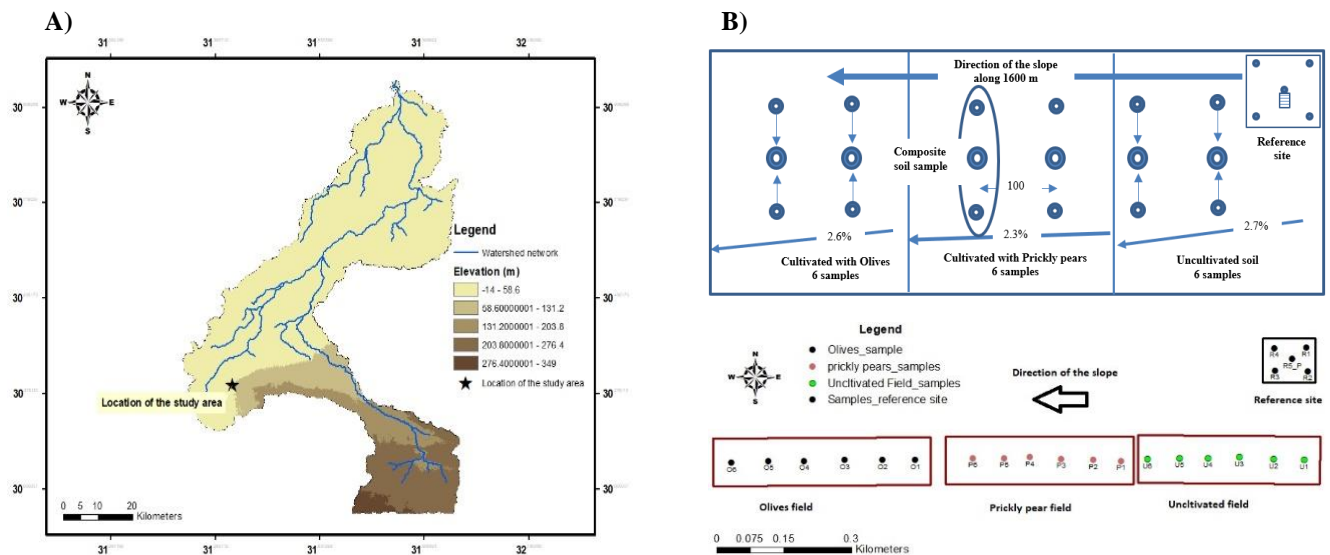


Fig. (1): A) Location of the study area, B) schematic representation and map of the study area where sampling strategy and slope of each area are illustrated for both the three fields and the reference site

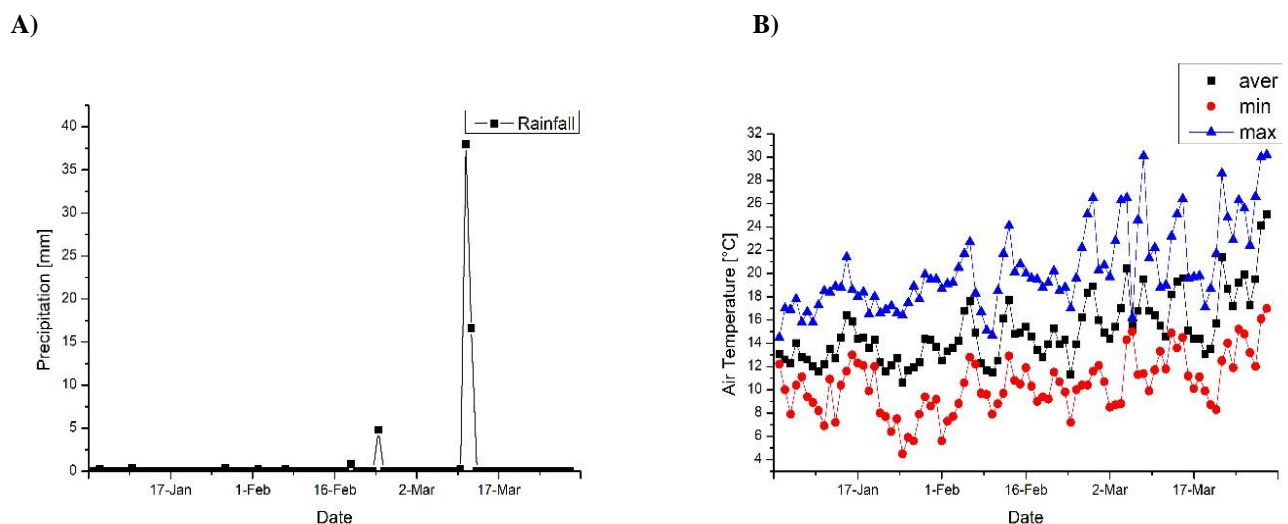


Fig. (2): A) Daily precipitation amount showing that intensive rainfall took place on March 11th and 12th 2020, B) daily average, minimum and maximum air temperature

A reference site located at a flat and undisturbed area and very close to studied fields. The soil samples at the reference site were taken from square grid of 25*25m, consists of 5 sampling points, 4 samples at the edge of the grid and one sample at the center. Samples were taken using a stainless-steel cylinder with dimensions of 40 cm diameter and height of 4 cm for core samples, while the depth increment soil samples in the center of the reference site were taken at sectioned core each 2 mm interval.

A transect strategy was adopted at the study area for each field. Each transect comprised 6 soil samples; the distance between each two constitutive samples is 60 m. A total of 18 composite soil samples was taken. Each composite sample comprised three soil cores collected in close proximity to capture local spatial variability. The texture of the study area was determined to be 'sandy' based on results from two samples at each location: one upslope and one downslope (Table 1).

Table (1): Some soil physical properties of the study area at the upstream and downstream of each field

Sample location	Depth	Particle size distribution %			Texture class	Bulk density
	0-20 cm	Sand	Silt	Clay		
Uncultivated Field	Upslope	96.8	2	1.2	Sand	1.60
	Downslope	94.5	3.8	1.7	Sand	1.55
prickly pear Field	Upslope	96	2.4	1.6	Sand	1.50
	Downslope	95.2	2.4	2.4	Sand	1.50
Olive field	Upslope	95.2	3.2	1.6	Sand	1.55
	Downslope	90	9	1.0	Sand	1.45

Preparing Soil Samples for Gamma Spectroscopy Inspection.

The soil samples were prepared for Gamma spectroscopy measurements according to the IAEA guidelines [31]. Each individual sample was air dried at 80 °C for 24 hours then it was grinded and sieved to ≤ 2 mm. The samples were homogenized and packed into cylindrical beakers sized 0.35 L suitable for Gamma analysis and the total weight of each sample was recorded.

The ^7Be activity concentration of the individual samples was measured using Broad energy HPGe gamma spectroscopy BE3830 model with cryostat CP5-PLUSE-SL and iPA-S1 preamplifier. FWHM: 450 eV at 5.9 keV, FWHM:750 eV at 122keV, FWHM, 1900 eV at 1332.5 keV) with a relative efficiency of 30% and shielded with Lead to minimize background. The detector is operated by Genie 2000 software and calibrated mathematically using LABSOCS based Monte Carlo software. The ^7Be activities were determined from the net area under full energy peak in the spectrum at 477.6 keV with counting time was set to 86400 seconds. The measured activities were decay corrected to the time of the sample collection.

Conversion of ^7Be Inventories to Estimates of Soil Redistribution Rates

Equations 1 and 2 can be used to convert the ^7Be activity concentration (Bq.kg^{-1}) into the total areal activity or inventory (Bq.m^{-2}) [31, 32]:

$$A_s = \frac{CM_t}{S} \quad \text{Eq. 1}$$

where:

C = activity of the analyzed sub-sample of the core sample (Bq.kg^{-1});

M_t = total mass of the whole core (kg);

S = area of the horizontal core cross section (m^2).

For the depth increment samples, the areal activity of ^7Be is expressed as:

$$A_s = \frac{1}{S} \sum_i M_{Ti} C_i \quad \text{Eq. 2}$$

where:

C_i = activity of the i^{th} sub-sample depth increment (Bq.kg^{-1});

M_{Ti} = total mass of the i^{th} sample depth increment (kg);

S = area of the horizontal core cross (m^2).

At the reference site, where the soil is undisturbed, it's supposed that the $z\text{Be}$ concentration $C(x)$ [Bq.kg^{-1}] has an exponential decline with soil mass depth x (positive downward) [kg m^{-2}]. Soil mass depth is used to measure the depth in soil and is obtained by multiplying soil bulk density and the depth of soil layer. Therefore, the activity concentration at a certain depth $C(x)$ can be expressed as in equation:(3)

$$C(x) = C(0)e^{\left(\frac{-x}{h_0}\right)} \quad \text{Eq. 3}$$

where $C(0)$ is the activity concentration on the soil surface. The parameter h_0 is the relaxation mass depth, which 63.2% of the ^7Be inventory can be found and is used to calculate the ^7Be penetration into soil and it relates ^7Be activity (Bq.kg^{-1}) with cumulative mass depth (Kg.m^{-2}). The exponential behavior of ^7Be concentration in undisturbed soils has been confirmed by many field experiments [8,9,27]

To estimate erosion or deposition in kg m^{-2} , we used the conversion model proposed by other

researchers [7, 22] to quantify the differences in ^7Be inventory between the reference sites and study sites .

Considering the distribution defined by Eq. (3), Changes in the sample site inventories can be represented as:

$$A(h) = \int_h^\infty C(x)dx = A_{ref} e^{\left(\frac{-h}{h_0}\right)} \quad \text{Eq. 4}$$

Erosion rates (kg.m^{-2}) can be estimated by comparing the ^7Be inventories at the sample site, A (kg.m^{-2}), to the reference inventory, A_{ref} (kg.m^{-2}). Where a mass of soil has been lost (h) (kg.m^{-2} , negative).

$$h = h_0 \ln\left(\frac{A}{A_{ref}}\right) \quad \text{Eq. 5}$$

Deposition of material is reflected in an excess of ^7Be inventory at the sample site with respect to the reference site. The depth of deposition, (h') (kg.m^{-2} , positive) can be calculated as:

$$h' = A - A_{ref}/C_d \quad \text{Eq. 6}$$

Where C_d (Bq.kg^{-1}) is the mean activity concentration of ^7Be in the deposited sediment .

RESULTS AND DISCUSSIONS

Reference Site

The results showed that reference site inventory was 124 ± 30 (Bq.m^{-2}), and the relaxation mass depth was estimated at 9.8 kg m^{-2} (equation 4). Considering the vertical distribution of ^7Be within soil profile, the measured distribution shows that the ^7Be is found in the upper layer reaching 14 mm of the soil profile (see figure 3B). This superficial distribution of ^7Be in soils has been found for other areas in arid regions [33, 34] and several

regions worldwide [27, 35]. Furthermore, it is observed that ^7Be activity shows an exponential decrease with increasing mass depth, and typically distribution of ^7Be in undisturbed soil (reference sites)

Soil Redistribution in the Studied Fields

The uncultivated field transect comprised composite samples, U1 to U6. The prickly pear field comprised 6 composite samples, P1 to P6, while the olive field samples were O1 to O6.

The measured ^7Be areal activity of each core ($A_{(x)}$) along each transect is shown in Table (2). The ^7Be inventories of the uncultivated field were lower than the reference inventory and it ranged from 59.9 to 122.5 ± 30 Bq.m^{-2} showing a 100% of water erosion process. For cultivated field by prickly pear, the ^7Be inventories ranged from 89.5 to 296.6 ± 30 Bq.m^{-2} showing erosion at both upstream and deposition process downstream. A similar behavior was observed at the cultivated field by olives where ^7Be inventories ranged from 73.9 to 263.6 ± 30 Bq.m^{-2} . The measured areal activity, the reference site inventory (A_{ref}) and the relaxation depth (h_0) were used in the profile distribution model to calculate both magnitudes of erosion (h) and deposition (h').

Erosion was dominant in the uncultivated field and the calculated gross erosion was 37 (t.ha^{-1}) and the net erosion was 37 (t.ha^{-1}) showing 100% of sediment delivery ratio due the intensive rain with the absence of ground cover. The variation in the ^7Be inventory within the transect could be linked to the transport of soil particles, with observed ^7Be , downslope due to the slope of the ground. Table (2) summarizes the results of soil redistribution processes for the three fields, uncultivated field and both cultivated with prickly pear and olives field..

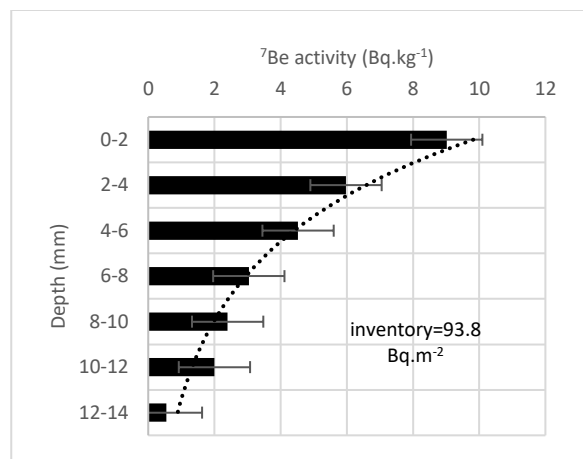
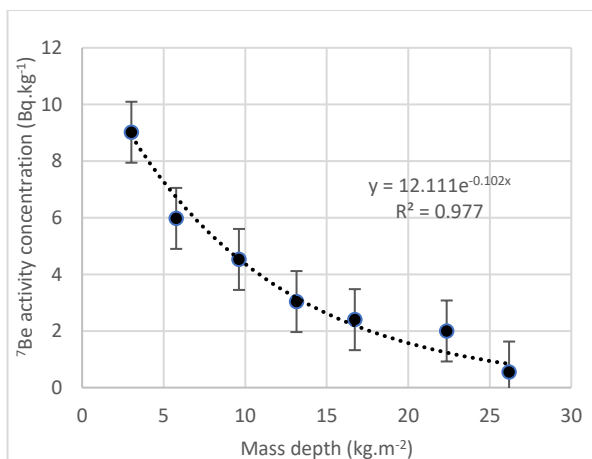


Fig. (3): ^7Be activity concentration (Bq.kg^{-1}) as a function of A) cumulative mass depth (kg.m^{-2}), B) depth (mm)

Table (2): Summary of Soil redistribution processes took place in the studied fields, erosion (h) / Deposition (h')

Transect No.	Sample No.	Elevation (m)	⁷ Be Inventory	Erosion (h)	Deposition (h')	In situ Process
			(Bq.m ⁻²)	(t. ha ⁻¹)	(t. ha ⁻¹)	
Uncultivated Field	U1	56	122.6	1.1	-	Erosion
	U2	54	98.5	22.5	-	Erosion
	U3	49	59.9	71.2	-	Erosion
	U4	47	92.2	29.1	-	Erosion
	U5	45	46.8	95.5	-	Erosion
	U6	44	121.1	2.3	-	Erosion
Prickly pears Field	P1	41	89.5	31.9	-	Erosion
	P2	39	123.6	0.3	-	Erosion
	P3	40	90.3	31.0	-	Erosion
	P4	35	122.4	1.3	-	Erosion
	P5	31	227.3	-	15.01	Deposition
	P6	29	296.6	-	25.07	Deposition
Olives field	O1	30	78.0	45.5	-	Erosion
	O2	28	74.0	50.6	-	Erosion
	O3	26	85.2	36.8	-	Erosion
	O4	23	126.3	-	0.23	Deposition
	O5	22	236.2	-	11.33	Deposition
	O6	21	263.8	-	14.12	Deposition

Concerning the prickly pear field, erosion process was observed in the upslope four sampling points P1, P2, P3 and P4, whereas deposition was observed at P5 and P6. The calculated gross erosion for prickly pears field was 10.8 (t.ha⁻¹) and the net erosion was 4.1 (t.ha⁻¹) showing 38% of sediment delivery ratio and these values are lower than other fields because the common slope in the prickly pears field was 2.3 % which is relatively lower than the common slope of the other two fields.

A similar behavior of soil redistribution was observed in the olive field where erosion was observed at the three upslope sampling points O1, O2 and O3, whereas

deposition was observed at the downstream for sampling points O4, O5 and O6. The calculated gross erosion for olives field was 22.2 (t.ha⁻¹) and the net erosion was 17.9 (t.ha⁻¹) showing 80% of sediment delivery ratio. The net erosion in Olives field is relatively higher than in Prickly Localization of erosion/deposition corresponding to each point is shown in Figure (4).

The soil redistribution process confirmed also by the increased percentage of both silt and clay particles found in soil samples taken at the upslope and downslope of each field, silt and clay contents were found to be higher in the downslope field than at upslope field as shown in Table 1.

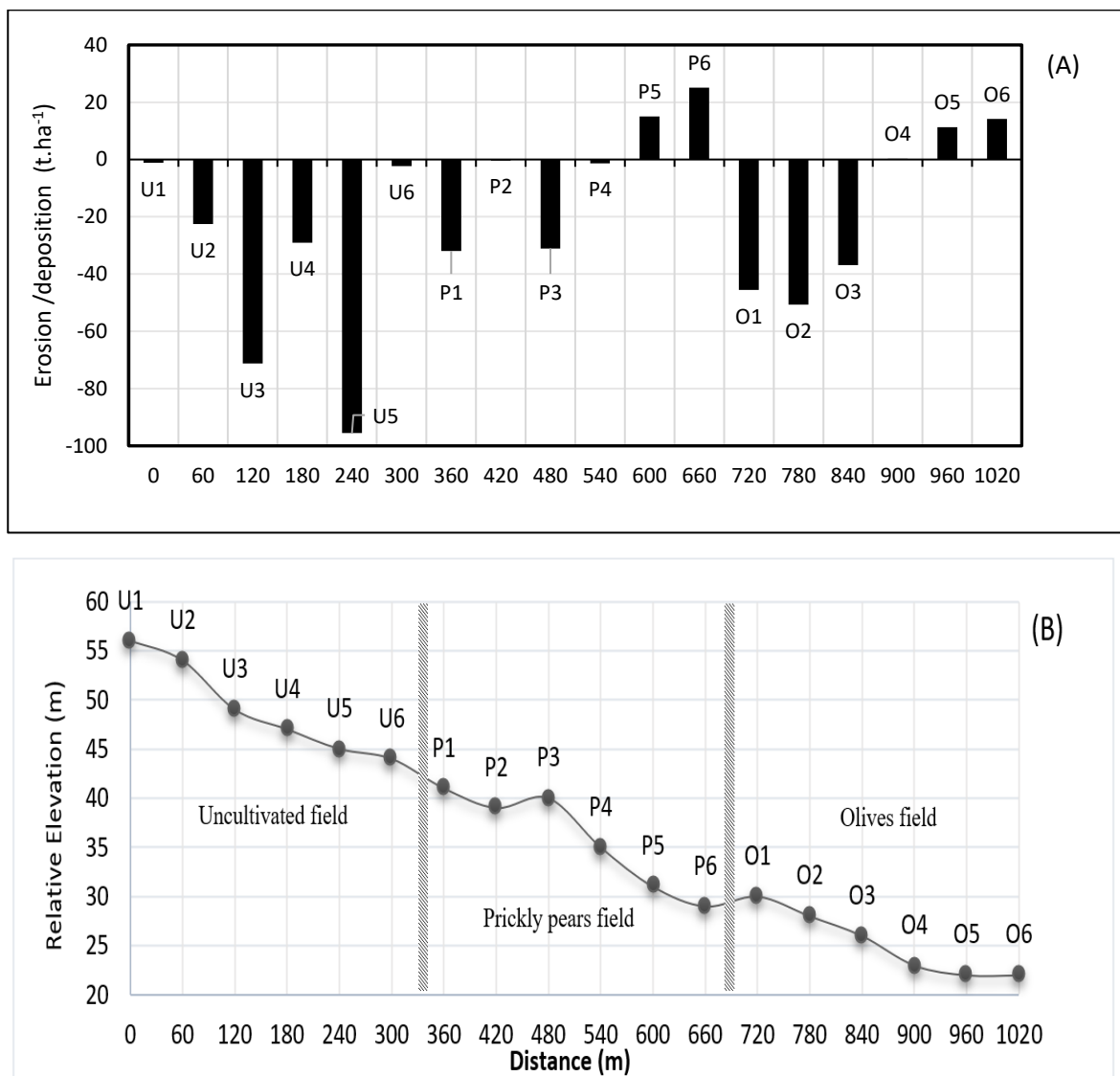


Fig. (4): A) Erosion and deposition for each point (t.ha⁻¹), negative values referrers to erosion and positive for deposition and B) relative elevation (m) across the three transects

The erosion process was globally observed at the study area including the three fields with gross erosion of 23.3 (t. ha⁻¹) and net erosion of 19.6 (t. ha⁻¹) showing 84% sediment delivery ratio.

The sheet erosion is globally ranked into several categories, according to mass of soil loss per unit area per year, insignificant erosion (< 0.5 m³.ha⁻¹), slight (weak) erosion (0.5- 5 t.ha⁻¹), moderate erosion (5-15 t.ha⁻¹), sever erosion (15-50 t.ha⁻¹), very severe erosion (50- 200 t.ha⁻¹) and catastrophic (>200 t.ha⁻¹) [36]. In Egypt, Mohamed et al. [37] studied the erosion hazard in the northern west coast, and they classified erosion risk into five classes, as; Non (< 2 t.ha⁻¹.y⁻¹), low

(4-10 t.ha⁻¹.y⁻¹), moderate (10-20 t.ha⁻¹.y⁻¹), high (20-30 t.ha⁻¹.y⁻¹) and very high (> 30 t.ha⁻¹.y⁻¹)

The ⁷Be technique estimates the erosion associated with a certain rain event, therefore the mass of soil eroded or deposited calculated by ⁷Be technique is attributed to the rainfall events that take place before the measurements. If the obtained soil erosion values are integrated to the year, this heavy rain which happened on 11th and 12th March 2020 could be taken as the main erosion events that cause erosion with the estimated erosion values of 37, 4.1 and 17.9 (t.ha⁻¹) for the uncultivated field, prickly pears and olives field, respectively. Combining the observed results and visual

observations at the three fields, the main driving force of soil erosion and deposition processes were the hillslopes and microtopography. The ^7Be technique would indicate that during this period, the soil loss values are in the range of low for cultivated field by prickly pears, moderate erosion for cultivated field by olives and severe erosion for uncultivated field according to the above-mentioned classification [37].

CONCLUSIONS

The performed study shows that the ^7Be technique can be used as a robust tool to estimate the soil erosion caused by rain, in an arid area due to relatively intensive rain event. For this research, three fields were chosen in a desertic area, the first field was uncultivated while the other two fields were cultivated by prickly pears.

A sampling campaign was performed for both the reference site and the three fields at the study area. Reference site measurements confirmed the validity of the reference site itself which shows an exponential decrease of ^7Be concentration with soil depth. In addition, the ability to measure the concentration of ^7Be in soil at different fields could be confirmed with the precision required by the technique.

The main results obtained showed that the ^7Be inventories of the uncultivated field were lower than the reference inventory and it ranged from 59.9 to 122.5 ± 30 Bq.m⁻² showing a 100% of water erosion process. For the cultivated field by prickly pear the ^7Be inventories ranged from 89.5 to 296.6 ± 30 Bq.m⁻² showing erosion at both upslope and deposition process downslope. A similar behavior was observed at the cultivated field by olives where ^7Be inventories ranged from 73.9 to 263.6 ± 30 Bq.m⁻². By applying the profile distribution conversion model, the obtained net erosion for the uncultivated field, prickly pears and olives field were 37, 4.1 and 17.9 (t.ha⁻¹) respectively. The erosion was caused by intensive rain event that took place on 11th and 12th March 2020 prior to the soil sampling. It could also be concluded that the prickly pear helps to preserve the soil from erosion in the significant rainfall event compared to olive cultivation and it could be a useful agricultural practice to combat erosion in that area.

It is not possible to compare the value of the erosion obtained with those reported for the region by other classical techniques, since these are reported as erosion rates per year. However, if the erosion value obtained could be extended to express the annual erosion rate, this area needs application of soil conservation to prevent

erosion and to restore soil especially for the uncultivated field.

ACKNOWLEDGEMENTS

This research was supported by IAEA/AFRA project RAF 5075 titled: Enhancing Regional Capacities for Assessing Soil Erosion and the Efficiency of Agricultural Soil Conservation Strategies through Fallout Radionuclides.

REFERENCES

- [1] Walling, D. E., He, Q., and Quine, T. A. (1995). Use of caesium-137 and lead-210 as tracers in soil erosion investigations. *Tracer technologies for hydrological systems. Proc. international symposium, Colorado*, 163–172.
- [2] Gallart, F., Llorens, P., and Latron, J. (1994). Studying the role of old agricultural terraces on runoff generation in a small Mediterranean mountainous basin. *J. of Hydro.*, 159(1), 291–303. [https://doi.org/https://doi.org/10.1016/0022-1694\(94\)90262-3](https://doi.org/https://doi.org/10.1016/0022-1694(94)90262-3)
- [3] Meliho, M., Noura, A., Benmansour, M., Boulmane, M., Khattabi, A., Mhammdi, N., and Benkdad, A. (2019). Assessment of soil erosion rates in Mediterranean cultivated and uncultivated soils using fallout ^{137}Cs . *J. of Envi. Radio.*, 208-209. <https://doi.org/10.1016/j.jenvrad.2019.106021>
- [4] Mullins, C. (2006). *Encyclopedia of Soil Science*, 2nd edition. Two Volumes. Edited by R. Lal. Boca Raton, FL, USA: CRC Press (2006), pp. 1923 36p Index, £340.00. ISBN 0-8493-3830-1. *Experimental Agriculture*, 42(4), 505–505. <https://doi.org/10.1017/S0014479706214108>
- [5] Mabit, L., Benmansour, M., and Walling, D. E. (2008). Comparative advantages and limitations of the fallout radionuclides ^{137}Cs , ^{210}Pb and ^7Be for assessing soil erosion and sedimentation. *J. of Envi. Radio.*, 99 (12), 1799–1807. <https://doi.org/10.1016/j.jenvrad.2008.08.009>
- [6] Schuller, P., Trumper, R. E., Sepúlveda-Varas, A., and Martín, A. (2000). Application of the ^{137}Cs technique to quantify soil redistribution rates in paleohumults from Central-South Chile. *Acta geológica hispánica, ISSN 0567-7505, Vol. 35, N° 3-4, 2000 (Ejemplar dedicado a: Assesment of soil erosion and sedimentation through the use of the ^{137}Cs and related techniques)*, pages. 285-290.

- [7] Walling, D. E., and He, Q. (1999). Improved Models for Estimating Soil Erosion Rates from Cesium-137 Measurements. *J. of Envi. Qual.*, 28(2),611–622. <https://doi.org/https://doi.org/10.2134/jeq1999.00472425002800020027x>
- [8] Walling, D. E., He, Q., and Zhang, Y. (2014). *Conversion Models And Related Software*. International Atomic Energy Agency (IAEA). Retrieved from http://www-pub.iaea.org/MTCD/Publications/PDF/TE-1741_web.pdf
- [9] Zapata, F., Garcia-Agudo, E., Ritchie, J. C., and Appleby, P. G. (2002). *Handbook for the Assessment of Soil Erosion and Sedimentation Using Environmental Radionuclides. Handbook for the Assessment of Soil Erosion and Sedimentation Using Environmental Radionuclides*. <https://doi.org/10.1007/0-306-48054-9>
- [10] Albergel, J., Collinet, J., Zante, P., and Hamrouni, H. (2011). Le rôle de la forêt méditerranéenne dans la conservation de l'eau et du sol. In *L'eau pour les forêts et les hommes en région méditerranéenne : un équilibre à trouver* (pp. 46–56). Joensuu: European Forest Institute. Retrieved from <https://www.documentation.ird.fr/hor/fdi:010065100>
- [11] Roose, E. (1993). Erosion...a current environmental problem ? The GCES, a new strategy for fighting erosion to resolve this dilemma of a growing society. In S. B. T.-F. L. E. WICHEREK (Ed.), (pp. 571–585). Amsterdam: Elsevier. <https://doi.org/https://doi.org/10.1016/B978-0-444-81466-1.50052-6>
- [12] Food and Agriculture Organization of the United Nations. (2019). *Use of 137Cs for Soil Erosion Assessment*. United Nations. Retrieved from <https://www.un-ilibrary.org/content/books/9789210040907>
- [13] Hu, J., Sha, Z., Wang, J., Du, J., and Ma, Y. (2020). Atmospheric deposition of 7Be, 210Pb in Xining, a typical city on the Qinghai-Tibet Plateau, China. *J. of Radio. and Nucl. Chem.*, 324. <https://doi.org/10.1007/s10967-020-07127-3>
- [14] Ródenas, C., Gómez-Arozamena, J., quindos poncela, L., Fernández, P., and Soto, J. (1997). 7Be concentrations in air, rain water and soil in Cantabria (Spain). *App. Rad. and Iso.*, 48, 545–548. [https://doi.org/10.1016/S0969-8043\(96\)00295-3](https://doi.org/10.1016/S0969-8043(96)00295-3)
- [15] Rosner, G., Hötzl, H., and Winkler, R. (1996). Continuous wet-only and dry-only deposition measurements of 137Cs and 7Be: An indicator of their origin. *App. Rad. and Iso.*, 47, 1135–1139. [https://doi.org/10.1016/S0969-8043\(96\)00119-4](https://doi.org/10.1016/S0969-8043(96)00119-4)
- [16] Ioannidou, A., and Papastefanou, C. (2006). Precipitation scavenging of 7Be and 137Cs radionuclides in air. *J. of Envi. Radio.*, 85, 121–136. <https://doi.org/10.1016/j.jenvrad.2005.06.005>
- [17] Yoshimori, M. (2005). Production and behavior of beryllium 7 radionuclide in the upper atmosphere. *Adv. in Space Res.*, 36(5), 922–926. <https://doi.org/https://doi.org/10.1016/j.asr.2005.04.093>
- [18] Liu, G., Wu, J., Li, Y., Su, L., and Ding, M. (2020). Temporal Variations of 7Be and 210Pb Activity Concentrations in the Atmosphere and Aerosol Deposition Velocity in Shenzhen, South China. *Aerosol and Air Quality Research*. <https://doi.org/10.4209/aaqr.2019.11.0560>
- [19] Asadov, A., and Krofcheck, D. (1999). Surface effect of cosmogenic 7Be concentration on macroscopic basalt. *J. of Envi. Radio.*, 46, 319–326. [https://doi.org/10.1016/S0265-931X\(98\)00150-7](https://doi.org/10.1016/S0265-931X(98)00150-7)
- [20] Doering, C., Akber, R., and Heijnis, H. (2006). Vertical distributions of Pb-210 excess, Be-7 and Cs-137 in selected grass covered soils in Southeast Queensland, Australia. *J. of Envi. Radio.*, 87, 135–147. <https://doi.org/10.1016/j.jenvrad.2005.11.005>
- [21] Taylor, A., Blake, W., and Keith-Roach, M. (2014). Estimating Be-7 association with soil particle size fractions for erosion and deposition modelling. *J. of Soils and Sedi.*, 14, 1886–1893. <https://doi.org/10.1007/s11368-014-0955-8>
- [22] Blake, W., Walling, D., and He, Q. (1999). Fallout beryllium-7 as a tracer in soil erosion investigations: including data, instrumentation and methods for use in agriculture, industry and medicine, *App. Rad. and Iso.*, 51 5, 599–605.
- [23] Daish, S., Dale, A. A., Dale, C., May, R., and Rowe, J. (2005). The temporal variations of 7Be, 210Pb and 210Po in air in England. *J. of Envi. Radio.*,84,457–467. <https://doi.org/10.1016/j.jenvrad.2005.05.003>

- [24] Dercon, G., Mabit, L., Hancock, G., Nguyen, M. L., Dornhofer, P., Bacchi, O. O. S., Zhang, X. (2012). Fallout radionuclide-based techniques for assessing the impact of soil conservation measures on erosion control and soil quality: An overview of the main lessons learnt under an FAO/IAEA Coordinated Research Project. *J. of Envi. Radio.*, 107, 78–85. <https://doi.org/10.1016/j.jenvrad.2012.01.008>
- [25] Kaste, J. M., Norton, S. A., and Hess, C. T. (2002). Environmental Chemistry of Beryllium-7. *Reviews in Mineralogy and Geochemistry - REV MINERAL GEOCHEM*, 50(1), 271–289. <https://doi.org/10.2138/rmg.2002.50.6>
- [26] Mabit, L., and Blake, W. (2019). *Assessing Recent Soil Erosion Rates through the Use of Beryllium-7 (Be-7)*. (L. Mabit and W. Blake, Eds.) *Assessing Recent Soil Erosion Rates through the Use of Beryllium-7 (Be-7)*. doi:10.1007/978-3-030-10982-0: Springer International Publishing. (pp. 1–61). <https://doi.org/10.1007/978-3-030-10982-0>
- [27] Sepúlveda-Varas, A., Schuller, P., Walling, D., and Castillo, A. (2008). Use of ⁷Be to document soil erosion associated with a short period of extreme rainfall. *J. of Envi. Radio.*, 99, 35–49. <https://doi.org/10.1016/j.jenvrad.2007.06.010>
- [28] Steinmann, P., Billen, T., Loizeau, J. L., and Dominik V. (1999). Beryllium-7 as a tracer to study mechanisms and rates of metal scavenging from lake surface waters. *J. Univ. de G. (Switzerland)* [https://doi.org/10.1016/S0016-7037\(99\)00021-6](https://doi.org/10.1016/S0016-7037(99)00021-6)
- [29] Wilson, C., Matisoff, G., and Whiting, P. (2003). Short-term erosion rates from a ⁷Be inventory balance. *Earth Surface Processes and Landforms - Earth Surf Process Landf*, 28, 967–977. <https://doi.org/10.1002/esp.509>
- [30] Kaste, J. M., Elmore, A., Vest, K., and Okin, G. (2011). Beryllium-7 in soils and vegetation along an arid precipitation gradient in Owens Valley, California. *Geo. Res Lett.*, 38. <https://doi.org/10.1029/2011GL047242>
- [31] IAEA. (2014). Guidelines for Using Fallout Radionuclides to Assess Erosion and Effectiveness of Soil Conservation Strategies. Vienna: International Atomic Energy Agency. Retrieved from <https://www.iaea.org/publications/10501/guidelines-for-using-fallout-radionuclides-to-assess-erosion-and-effectiveness-of-soil-conservation-strategies>
- [32] Petrović, J., Dragović, S., Dragović, R., Dordević, M., Dokić, M., Zlatković, B., and Walling, D. (2016). Using ¹³⁷Cs measurements to estimate soil erosion rates in the Pčinja and South Morava River Basins, southeastern Serbia. *J. of Envi. Radio.*, 158–159, 71–80. <https://doi.org/10.1016/j.jenvrad.2016.04.001>
- [33] Lohaiza, F., Velasco, H., Juri Ayub, J., Rizzotto, M., Di Gregorio, D., Huck, H., and Valladares, D. (2014). Annual variation of Be-7 soil inventory in a semiarid region of central Argentina. *J. of Envi. Radio.*, 130C, 72–77. <https://doi.org/10.1016/j.jenvrad.2014.01.006>
- [34] de Rosas, J. P., Esquivel López, A., Heimann, D., Negri, A., Lohaiza, F., Valladares, D., and Ayub, J. (2018). Using beryllium-7 to evaluate soil erosion processes in agricultural lands in semiarid regions of Central Argentina. *Envi. Eart Sci.*, 77, 587. <https://doi.org/10.1007/s12665-018-7767-x>
- [35] Schuller, P., Iroumé, A., Walling, D., Mancilla, H., Castillo, A., and Trumper, R. (2006). Use of Beryllium-7 to Document Soil Redistribution Following Forest Harvest Operations. *J. of envi. qual.*, 35, 1756–1763. <https://doi.org/10.2134/jeq2005.0410>
- [36] Zachar, D. B. T.-D. in S. S. (Ed.). (1982). Chapter 2 Classification of Soil Erosion. In *Soil Erosion*. 10 (27–136). Elsevier. [https://doi.org/https://doi.org/10.1016/S0166-2481\(08\)70645-7](https://doi.org/https://doi.org/10.1016/S0166-2481(08)70645-7)
- [37] Mohamed, E. . S., Schütt, B., and Belal, A. (2013). Assessment of environmental hazards in the north western coast -Egypt using RS and GIS. *Egyptian J. of Rem. Sens. and Space Sci.*, 16(2), 219–229. <https://doi.org/10.1016/j.ejrs.2013.11.003>